КВАНТОВЫЕ КОММУНИКАЦИИ С КОДИРОВАНИЕМ В НЕПРЕРЫВНЫХ ПЕРЕМЕННЫХ

УДК 535.14

CONTINUOUS VARIABLE TRIPARTITE ENTANGLEMENT AND EINSTEIN–PODOLSKY–ROSEN CORRELATIONS FROM TRIPLE NONLINEARITIES

© 2007 г. M. K. Olsen, A. S. Bradley, and M. D. Reid

ARC Centre of Excellence for Quantum-Atom Optics, School of Physical Sciences, University of Queensland, Brisbane, Qld 4072, Australia

E-mail: mko@physics.uq.edu.au

Received October 12, 2006

Abstract—We develop three-mode generalisations of the Einstein–Podolsky–Rosen paradox, allowing us to define inequalities which may be used to indicate continuous-variable tripartite entanglement. We use these inequalities and an appropriate version of the previously developed van Loock–Furusawa inequalities to theoretically compare the continuous-variable tripartite entanglement available from the use of three concurrent $\chi^{(2)}$ nonlinearities and from three independent squeezed states mixed on beamsplitters.

PACS: 42.50.Dv, 42.65.Lm, 03.65.Ud

INTRODUCTION

One of the central properties which distinguishes quantum mechanics from classical mechanics is that of entanglement. Measurable continuous-variable bipartite entanglement is readily producible experimentally and there has been some progress in the production of tripartite entangled beams, with the entanglement often obtained by mixing squeezed vacua with linear optical elements [1, 2]. Other methods which create the entanglement in the actual nonlinear interaction have been proposed and are under investigation, using both cascaded and concurrent $\chi^{(2)}$ processes [3–7]. In the present work we investigate the achievable tripartite entanglement available from both the use of three concurrent $\chi^{(2)}$ nonlinearities and three independent squeezed states mixed on beamsplitters, using an appropriate version of the van Loock–Furusawa inequalities. We also develop and use three-mode generalisations of the Einstein–Podolsky–Rosen (EPR) paradox [8] which are an alternative for demonstrating the inseparability of the system density matrix.

A two-mode system is considered to be bipartite entangled if the system density matrix cannot be expressed as a product of density matrices for each of the two modes. The definition of tripartite entanglement for three-mode systems is more subtle, with different classes of entanglement having been defined, depending on how the system density matrix may be partitioned [9]. The classifications range from fully inseparable, which means that the density matrix is not separable for any grouping of the modes, to fully separable, where the three modes are not entangled in any way. For the fully inseparable case, van Loock and Furusawa[10], who call this genuine tripartite entanglement, have derived entanglement criteria in terms of inequalities which are experimentally measurable for continuous variable processes. In this work we analyse two different systems in terms of these inequalities, as well as in terms of our three-mode EPR criteria. We note here that both these methods of detecting entanglement provide sufficient, but not necessary, conditions, so that one or the other may be more sensitive and/or useful in a given situation.

CRITERIA FOR TRIPARTITE ENTANGLEMENT

Genuine tripartite entanglement is verified if we rule out any bipartition of the density matrix ($\hat{\rho}$), which is to say that the full system density matrix cannot be expressed in any of the following forms

$$\hat{\rho} = \sum_r \hat{\rho}_r^{12}\hat{\rho}_r^{3}, \quad \hat{\rho} = \sum_r \hat{\rho}_r^{1}\hat{\rho}_r^{23}, \quad \hat{\rho} = \sum_r \hat{\rho}_r^{13}\hat{\rho}_r^{2}, \quad (1)$$

where 1, 2 and 3 are the mode indices. If these factorisations are ruled out then so is the fully separable form $\hat{\rho} = \sum_r \hat{\rho}_r^1\hat{\rho}_r^2\hat{\rho}_r^3$.

The van Loock–Furusawa Inequalities

We will first review known inequalities which, if violated, demonstrate that a system exhibits true continuous variable tripartite entanglement according to the above definition. For three modes described by the annihilation operators $\hat{a}_j$, where j = 1, 2, 3, we define quadrature operators for each mode as

$$\hat{X}_j = \hat{a}_j + \hat{a}_j^\dagger, \quad \hat{Y}_j = -i(\hat{a}_j - \hat{a}_j^\dagger), \quad (2)$$

so that the Heisenberg uncertainty principle requires $V(\hat{X}_j)V(\hat{Y}_j) \geq 1$. A set of conditions which are sufficient to demonstrate tripartite entanglement for any quantum state have been derived by van Loock and Furusawa [10]. Using our quadrature definitions, the van Loock–Furusawa conditions give a set of inequalities,

$$\begin{aligned} V_{12} &= V(\hat{X}_1 - \hat{X}_2) + V(\hat{Y}_1 + \hat{Y}_2 + g_3\hat{Y}_3) \geq 4, \\ V_{13} &= V(\hat{X}_1 - \hat{X}_3) + V(\hat{Y}_1 + g_2\hat{Y}_2 + \hat{Y}_3) \geq 4, \\ V_{23} &= V(\hat{X}_2 - \hat{X}_3) + V(g_1\hat{Y}_1 + \hat{Y}_2 + \hat{Y}_3) \geq 4, \end{aligned} \tag{3}$$

where $V(A) \equiv \langle A^2 \rangle - \langle A \rangle^2$. As shown in Ref. [10], if any two of these inequalities are violated, the system is fully inseparable and genuine tripartite entanglement is guaranteed. We note that genuine tripartite entanglement may still be possible when none of these inequalities is violated, due to the criteria being sufficient but not necessary. We also note here that the interaction Hamiltonians of the systems which we evaluate in this work are symmetric under mode permutations if the $\chi^{(2)}$ interactions are of equal strength, and by setting the input fields equal, we need only consider the case where $g_1 = g_2 = g_3 = 1$, although in general this will not be the case. In fact, the inequalities in the form we use here are suitable, optimal and sufficient for our purposes.

Entanglement and Einstein–Podolsky–Rosen Correlations

In 1989 Reid [11], and Reid and Drummond [12] proposed a physical test of the EPR paradox using optical quadrature amplitudes, which are mathematically identical to the position and momentum originally considered by EPR. Reid later expanded on this work, demonstrating that the satisfaction of the 1989 two-mode EPR criterion always implies bipartite quantum entanglement [13]. It was also shown by Tan [14] that the possible definition of two orthogonal quadratures, the product of whose variances violates the limits set by the Heisenberg uncertainty principle (HUP), provides evidence of entanglement. In this work we extend Reid's original approach, based on an inferred HUP between two quadratures, to the case of tripartite correlations, where quadratures of three different optical modes are involved. We find that there is more than one way to define EPR correlations for a system exhibiting tripartite entanglement. We have used two of the possible methods in a previous publication [5], while Bowen *et al.* have defined a third [15]. In this work we will use the correlations we defined previously to demonstrate the presence of tripartite entanglement.

There are two forms of the criteria that we need to consider, arising from one and two mode inference. The first inference scheme that we will use to prove tripartite entanglement and EPR correlations involves using experimental observations of two modes to infer properties of a third. The proof for this scheme is essentially the same as for the original bipartite entanglement result of [13] and has been detailed in [7]. In practice one usually has access to certain moments of quadrature variables, in particular, the elements of the covariance matrix. Hence we can find sufficent conditions for entanglement which may be of great practical value, in that experiments have been performed to measure their bipartite versions [16] and can be generalised to the tripartite case without undue difficulty.

To begin, we make a linear estimate $\hat{X}_{i,\,\mathrm{est}}$ of the quadrature $\hat{X}_i$ for the mode i from the properties of the combined mode $j + k$, so that, for example

$$\hat{X}_{i,\,\mathrm{est}} = a(\hat{X}_j \pm \hat{X}_k) + c, \tag{4}$$

where a and c are parameters which can be optimised, both experimentally and theoretically [11, 16]. It has been shown [12] that this corresponds to minimising the variance

$$\begin{aligned} &V_{\mathrm{est}}^{\mathrm{inf}}(\hat{X}_i - a(\hat{X}_j \pm \hat{X}_k)) = \\ &= \langle (\hat{X}_i - a(\hat{X}_j \pm \hat{X}_k))^2 \rangle - \langle \hat{X}_i - a(\hat{X}_j \pm \hat{X}_k) \rangle^2 \end{aligned} \tag{5}$$

with respect to a. The minimum is achieved when

$$a_{\min} = \frac{V(\hat{X}_i, \hat{X}_j \pm \hat{X}_k)}{V(\hat{X}_j \pm \hat{X}_k)}. \tag{6}$$

In the above $V(\hat{A}, \hat{B}) = \langle \hat{A}\hat{B} \rangle - \langle \hat{A} \rangle \langle \hat{B} \rangle$. Defining the optimal inferred variance for $\hat{X}_i$ as $V^{\mathrm{inf}}(\hat{X}_i) \equiv \equiv V_{\mathrm{est}}^{\mathrm{inf}}(\hat{X}_i)\big|_{a = a_{\min}}$, we obtain

$$V^{\mathrm{inf}}(\hat{X}_i) = V(\hat{X}_i) - \frac{[V(\hat{X}_i, \hat{X}_j \pm \hat{X}_k)]^2}{V(\hat{X}_j \pm \hat{X}_k)}. \tag{7}$$

We follow the same procedure for the $\hat{Y}$ quadratures to give expressions which may be obtained by swapping each $\hat{X}$ for a $\hat{Y}$ in the above to give the optimal inferred estimate

$$V^{\mathrm{inf}}(\hat{Y}_i) = V(\hat{Y}_i) - \frac{[V(\hat{Y}_i, \hat{Y}_j \pm \hat{Y}_k)]^2}{V(\hat{Y}_j \pm \hat{Y}_k)}. \tag{8}$$

A demonstration of the EPR paradox can be claimed whenever it is observed that $V_{\mathrm{est}}^{\mathrm{inf}}(\hat{X}_i)V_{\mathrm{est}}^{\mathrm{inf}}(\hat{Y}_i) < 1$, and we have shown that such an experimental outcome is possible whenever the theory predicts

$$V^{\mathrm{inf}}(\hat{X}_i)V^{\mathrm{inf}}(\hat{Y}_i) < 1. \tag{9}$$

This demonstration for the 3 possible values of i is then sufficient to establish genuine tripartite entanglement.

Our alternative scheme uses information about one mode to infer the combined properties of the other two. In this case one measures $V_{\mathrm{inf}}(\hat{X}_j \pm \hat{X}_k) = V_{\mathrm{est}}^{\mathrm{inf}}(\hat{X}_j \pm \hat{X}_k -$

$-a\hat{X}_i)|_{a = a_{\min}}$. Linear inference leads to the expression for the optimal (minimum) variance in the inferred quadrature $\hat{X}_j + \hat{X}_k$

$$V^{\inf}(\hat{X}_j \pm \hat{X}_k) = \\ = V(\hat{X}_j \pm \hat{X}_k) - \frac{[V(\hat{X}_i, \hat{X}_j) \pm V(\hat{X}_i, \hat{X}_k)]^2}{V(\hat{X}_i)}, \quad (10)$$

which is merely a different form of the expression given in Ref. [5],

$$V^{\inf}(\hat{X}_j \pm \hat{X}_k) = \\ = V(\hat{X}_j \pm \hat{X}_k) - \frac{[V(\hat{X}_i, \hat{X}_j \pm \hat{X}_k)]^2}{V(\hat{X}_i)}. \quad (11)$$

The same expressions hold for the Y quadratures, and it is then straightforwardly shown that the HUP requires that

$$V(\hat{X}_j \pm \hat{X}_k)V(\hat{Y}_j \pm \hat{Y}_k) \geq 4. \quad (12)$$

There is thus a demonstration of this three mode form of the EPR paradox whenever $V_{\text{est}}^{\inf}(\hat{X}_j \pm \hat{X}_k)V_{\text{est}}^{\inf}(\hat{Y}_j \pm \hat{Y}_k) < 4$, which is predicted to be possible when

$$V^{\inf}(\hat{X}_j \pm \hat{X}_k)V^{\inf}(\hat{Y}_j \pm \hat{Y}_k) < 4. \quad (13)$$

As above, this demonstration for the 3 possible combinations also serves to establish complete inseparability of the density matrix.

ENTANGLEMENT VIA BEAMSPLITTERS

It is simple to show that one quadrature squeezed state, with squeezing parameter r, mixed on a beamsplitter with a vacuum input, results in a bipartite entangled state with a value of $2(1 + e^{-r})$ for the Duan criterion [17] for bipartite entanglement (see also Simon [18]), where a value of less than 4 represents bipartite entanglement. If an amplitude squeezed state is mixed with a phase-squeezed state on a beamsplitter, both with squeezing parameter r, this gives a value of $4e^{-r}$ for the same criterion. In this section we will quantify one possible way in which tripartite entanglement may be obtained, using squeezed states obtained from individual $\chi^{(2)}$ processes, which are subsequently combined utilising beamsplitters.

A schematic of an apparatus which has been used by Aoki *et al.* [2] to produce tripartite entanglement by this method is given in Fig. 1, showing the three optical parametric oscillators (OPO) and the two beamsplitters used. They experimentally measured continuous variable tripartite entanglement, obtaining values for the criteria of (3) which were just above 3 using our quadrature definitions. To perform a realistic analysis of this scheme we must consider that OPOs do not produce minimum uncertainty squeezed states with a monotonically increasing squeezing parameter, but exhibit quite different behaviours above and below the oscillation threshold. Here we consider output quadrature amplitudes at a particular frequency ω, so that, following Collett and Gardiner [19], we define the associated spectral quadratures $\hat{X}_j(\omega)$ and $\hat{Y}_j(\omega)$, $j = 1, 2, 3$, and the associated spectral variances. This then means that we can define $S^{\inf}(\hat{X}_i)$, for example, as the inferred spectral variance corresponding to $V^{\inf}(\hat{X}_i)$ and so on. We will consider an OPO where $\hat{a}$ and $\hat{b}$ represent the signal and pump modes, with respective cavity dampings γ_a and γ_b. With the classical pump represented by ϵ and the effective nonlinearity by κ, we find that there is a critical threshold pump value $\epsilon_c = \gamma_a\gamma_b/\kappa$, below which the signal mode is not macroscopically occupied. The output spectra for this OPO system are well known [19], with the below threshold spectral variances for mode $\hat{a}$ being

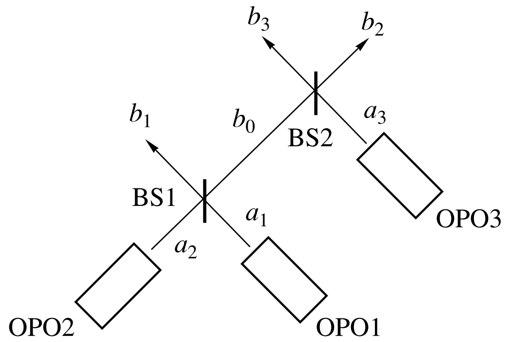

Fig. 1. The Aoki scheme, which mixes three squeezed states on two beamsplitters with different reflectivities. BS1 has reflectivity μ and BS2 has reflectivity ν.

$$S^{\text{out}}(\hat{X}_a) = 1 + \frac{4\gamma_a\gamma_b\kappa\epsilon}{(\gamma_a\gamma_b - \kappa\epsilon)^2 + \gamma_b^2\omega^2}, \\ S^{\text{out}}(\hat{Y}_a) = 1 - \frac{4\gamma_a\gamma_b\kappa\epsilon}{(\gamma_a\gamma_b + \kappa\epsilon)^2 + \gamma_b^2\omega^2}, \quad (14)$$

while above threshold they are

$$S^{\text{out}}(\hat{X}_a) = 1 + \frac{4\gamma_a^2(\gamma_b^2 + \omega^2)}{(2\gamma_a\gamma_b - 2\kappa\epsilon + \omega^2)^2 + \gamma_b^2\omega^2}, \\ S^{\text{out}}(\hat{Y}_a) = 1 - \frac{4\gamma_a^2(\gamma_b^2 + \omega^2)}{(\omega^2 - 2\kappa\epsilon)^2 + (2\gamma_a + \gamma_b)^2\omega^2}. \quad (15)$$

The output field $\hat{a}$ exhibits squeezing and three such outputs of three OPOs are used as the inputs $\hat{a}_1$, $\hat{a}_2$, $\hat{a}_3$ of Fig. 1. We note here that, as the results (14) and (15) are derived using a linearised fluctuation analysis, they are not valid in the immediate region of the threshold.

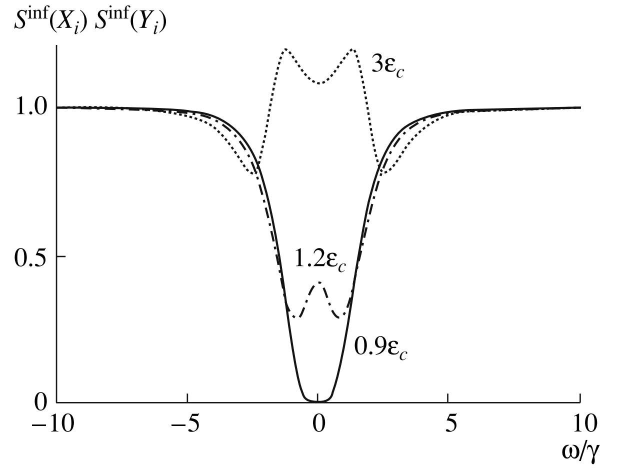

Fig. 2. The EPR spectral correlations, $S^{inf}(\hat{X}_i)S^{inf}(\hat{Y}_i)$ of the Aoki scheme, for different ratios of the pumping rates to the critical threshold pumping rate. We have set $\mu = 2/3$, $\nu = 1/2$, and the outputs are calculated via a linearised fluctuation analysis of the standard OPO equations, with $\gamma_a = \gamma_b = 1$ and $\kappa = 10^{-2}$. The three curves are for different ratios of the pumping rates to the critical threshold pumping rate. All three correlations are equal for these parameters. The value $S_{ij} = 1$ defines the upper boundary for true tripartite entanglement.

Following Reid and Drummond [12], it is possible to use these expressions as inputs to calculate the EPR correlations in the spectral domain.

In Fig. 2 we show results for the inference of one quadrature from a combination of the other two, for the system of Aoki *et al.* [2]. In this case, a value of $S^{inf}(\hat{X}_i)S^{inf}(\hat{Y}_j) < 1$ indicates EPR correlations, and therefore genuine tripartite entanglement. The results for inferring the combined quadratures from the single ones are found in this case by multiplying the results of Fig. 2 by 4, replacing, for example the $S^{inf}(\hat{X}_1)S^{inf}(\hat{Y}_1)$ with $S^{inf}(\hat{X}_2 \pm \hat{X}_3)S^{inf}(\hat{Y}_2 \pm \hat{Y}_3)$ and noting that the upper bound for EPR correlations is then 4. We see that this system demonstrates entanglement and the EPR paradox for a wide range of pumping strengths, these correlations persisting well into the region where the output fields are relatively intense and truly macroscopic.

ENTANGLEMENT VIA THREE CONCURRENT INTRACAVITY NONLINEARITIES

We now turn our attention to a process in which the entanglement is produced in a single nonlinear interaction which combines three concurrent nonlinearities. The system we investigate in this section is derived from work by Pfister *et al.* [20], who raised the possibility of concurrent parametric down conversion in a single optical parametric amplifier (OPA). They also gave some solutions for equations of motion derived directly from the interaction Hamiltonian in the undepleted pump approximation, as well as experimentally observing triply coincident nonlinearities in periodically poled $KTiOPO_4$ [21].

The system has three inputs which interact with the crystal to produce three output beams at frequencies ω_0, ω_1 and ω_2, which may be equal. The interactions are selected to couple distinct polarisations, and the scheme relies on tuning the field strengths in order to compensate for differences in the susceptibilities since it is usually the case that $\chi_{yzy} \neq \chi_{zzz}$. Note that x is the axis of propagation within the crystal. The mode described by $\hat{b}_1$ is pumped at frequency and polarisation $(\omega_0 + \omega_1, y)$ to produce the modes described by $\hat{a}_1(\omega_0, z)$ and $\hat{a}_2(\omega_1, y)$, the mode described by $\hat{b}_2$ is pumped at $(\omega_1 + \omega_2, y)$ to produce the modes described by $\hat{a}_2$ and $\hat{a}_3(\omega_2, z)$, while the mode described by $\hat{b}_3$ is pumped at $(2\omega_1, z)$ to produce the modes described by $\hat{a}_1$ and $\hat{a}_2$. The interaction Hamiltonian for the six-mode system is then

$$H_{\text{int}} = i\hbar(\chi_1\hat{b}_1\hat{a}_1^\dagger\hat{a}_2^\dagger + \chi_2\hat{b}_2\hat{a}_2^\dagger\hat{a}_3^\dagger + \chi_3\hat{b}_3\hat{a}_1^\dagger\hat{a}_3^\dagger) + \text{h.c.},\qquad(16)$$

with the χ_j representing the effective nonlinearities. In what follows, we will set $\chi_j = \chi$ and the high frequency input intensities as equal, with vacuum inputs at the lower frequencies. These are the conditions that we have previously found to give maximum violation of the entanglement inequalities.

The experimentally realistic case where this interaction takes place inside a pumped Fabry–Perot cavity, has been previously investigated theoretically by Bradley *et al.* [5] and is currently under experimental investigation by Pfister *et al.* [22]. In the best case, where the three pumping inputs and nonlinearities are equal, relatively simple analytic expressions can be found for the output spectral correlations equivalent to (3) by following the usual linearised fluctuation analysis procedure. We make the proviso that these are not valid in the immediate region of the oscillation threshold, which occurs at a pump amplitude of $\epsilon^{th} = \gamma\kappa/2\chi$, where γ is the cavity damping rate at the high frequencies and κ is the low-frequency damping rate. Below threshold, the steady-state solutions for the α_j are all zero, while $\beta_j^{ss} = \epsilon/\gamma$. Above threshold these solutions become $\beta_j^{ss} = \kappa/2\chi$ and $\alpha_j^{ss} = \sqrt{(\epsilon - \epsilon^{th})/\chi}$. We note here that, due to the presence of the square-root, there is an ambiguity in the sign of these solutions. However, closer analysis shows that all must have the same sign, whether this is positive or negative. The full spectral correlations have been presented in [5] for the damping ratio $\gamma/\kappa = 10$ in which case the maximum violation of the van Loock–

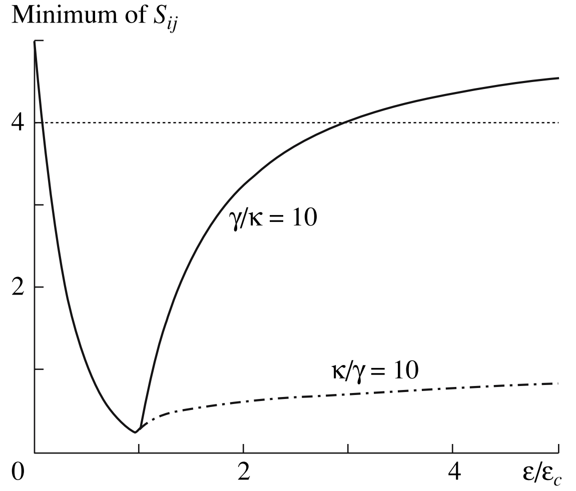

Fig. 3. The S_{ij} correlations as a function of the ratio of the cavity pumping to the threshold value and for different ratios of the cavity damping rates for the intracavity triply concurrent scheme. The dashed line at 4 defines the upper boundary for true tripartite entanglement. The parameter values for the solid line were $\gamma = 10$, $\kappa = 1$ and $\chi = 10^{-2}$, and for the dash-dotted line, $\gamma = 1$, $\kappa = 10$ and $\chi = 10^{-2}$.

Furusawa inequalities is found at zero frequency. These zero-frequency correlations are then found as (where S_{ij} corresponds to the spectral output equivalent of V_{ij} inside the cavity)

$$\begin{aligned} S_{ij}^{\text{below}}(0) &= 5 - \frac{8\kappa\gamma\chi\epsilon(4\kappa^2\gamma^2 + 10\kappa\gamma\chi\epsilon + 7\chi^2\epsilon^2)}{(\kappa\gamma + \chi\epsilon)^2(\kappa\gamma + 2\chi\epsilon)^2}, \\ S_{ij}^{\text{above}}(0) &= 5 - \frac{\kappa^2\gamma^2(3\kappa^2\gamma^2 + 6\kappa\gamma\chi\epsilon + 19\chi^2\epsilon^2)}{4\chi^2\epsilon^2(\kappa\gamma + \chi\epsilon)^2}. \end{aligned} \tag{17}$$

When the damping ratio is changed so that $\kappa/\gamma = 10$, the below threshhold results are unchanged, but above threshold the spectra bifurcate so that the maximum violation is found at non-zero frequencies. In Fig. 3 we present the minimum of the correlation functions (maximum violation of the inequalities) for each of these cases. It is immediately obvious that the entanglement persists much further above threshhold in the bifurcated case. As this is no longer close to zero frequency, where technical noise can be a real problem, this may be a real operational advantage

The expressions for the EPR correlations are rather more unwieldy and it is therefore not practical to give these here. They are plotted for various ratios of the pumping to the critical pumping rate in Fig. 4 and Fig. 5. In the results of Fig. 4, $\gamma = 10\kappa$ and we find that the violation of the inequalities disappears rapidly above the threshhold pumping value. On the other hand, when $\kappa = 10\gamma$, as shown in Fig. 5, the spectra bifurcate and a large degree of violation is found in the sidebands at well above threshhold. We also note here that, above threshold, the output modes are macroscopically occupied, with intensities $|\alpha_j|^2 = (\epsilon - \epsilon^{\text{th}})/\chi$, so that, especially for the case with $\kappa > \gamma$, genuine continuous-variable tripartite entanglement is potentially available with intense outputs.

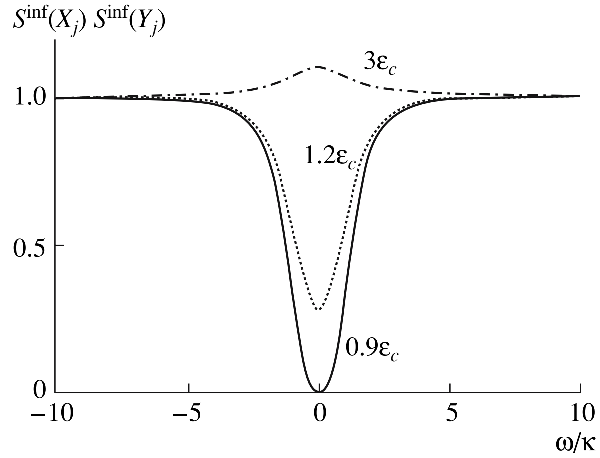

Fig. 4. The spectral EPR correlations for different ratios of the pumping rate to the critical pumping rate, for the intracavity triply concurrent scheme. The parameter values are $\gamma = 10$, $\kappa = 1$ and $\chi = 10^{-2}$.

CONCLUSIONS

We have examined two different interaction schemes in terms of their potential as sources of continuous variable tripartite entanglement, in terms of both the well-known van Loock–Furusawa correlations and two three-mode EPR criteria which we have developed. We find that both give broadly similar results for the specific cases we have examined here as there is a symmetry which makes a simple choice of the quadrature combinations possible. This may not always be the case

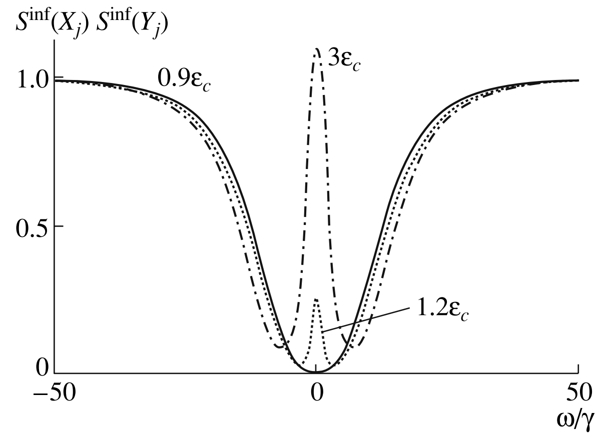

Fig. 5. The spectral EPR correlations correlations for different ratios of the pumping rate to the critical pumping rate, for the intracavity triply concurrent scheme. The parameter values are $\gamma = 1$, $\kappa = 10$ and $\chi = 10^{-2}$.

for an arbitrary system. As for the actual schemes, we have shown that the one which mixes the outputs of three OPOs on beamsplitters and that in which the three entangled modes are created in the one intracavity nonlinear material have similar performance except in the far above threshold region. Which of these two schemes is preferable for practical purposes would seem to depend more on the robustness of the experimental setup and the preferences of individual experimentalists rather than any inherent advantages that either may have. On the one hand, individual OPOs are familiar technology while the type of crystal needed for the concurrent scheme is relatively new technology. On the other hand, it may prove easier to stabilise one cavity rather than having to simultaneously stabilise and synchronise three OPOs.

ACKNOWLEDGMENTS

This research was supported by the Australian Research Council and the Queensland state government. We thank Sergei Kilin for the opportunity to present this work at the ICQO'2006 conference in Minsk.

REFERENCES

1. J. Jing, J. Zhang, Y. Yan, F. Zhao, C. Xie, and K. Peng, Phys. Rev. Lett. **90**, 167903 (2003).
2. T. Aoki, N. Takei, H. Yonezawa, K. Wakui, T. Hiraoka, and A. Furusawa, Phys. Rev. Lett. **91**, 080404 (2003).
3. J. Guo, H. Zou, Z. Zhai, J. Zhang and J. Gao, Phys. Rev. A **71**, 034305 (2005).
4. A. Ferraro, M. G. A. Paris, M. Bondani, A. Allevi, E. Puddu, and A. Andreoni, J. Opt. Soc. Am. B **21**, 1241 (2004).
5. A. S. Bradley, M. K. Olsen, O. Pfister, and R. C. Pooser, Phys. Rev. A **72**, 053805 (2005).
6. M. K. Olsen and A. S. Bradley, J. Phys. B **39**, 127 (2006).
7. M. K. Olsen, A. S. Bradley, and M. D Reid, **39**, 2515 (2006).
8. A. Einstein, B. Podolsky, and N. Rosen, Phys. Rev. **47**, 777 (1935).
9. G. Giedke, B. Kraus, M. Lewenstein, and J. I. Cirac, Phys. Rev. A **64**, 052303 (2001).
10. P. van Loock and A. Furusawa, Phys. Rev. A **67**, 052315 (2003).
11. M. D. Reid, Phys. Rev. A **40**, 913 (1989).
12. M. D. Reid and P. D. Drummond, Phys. Rev. A **40**, 4493 (1989).
13. M. D. Reid, in Quantum Squeezing, Ed. by P. D. Drummond and Z. Ficek (Springer, Berlin, 2004), pp. 337–362.
14. S. M. Tan, Phys. Rev. A **60**, 2752 (1999).
15. W. P. Bowen, P. K. Lam, and T. C. Ralph, J. Mod. Opt. **50**, 801 (2003).
16. Z. Y. Ou, S. F. Pereira, H. J. Kimble, and K. C. Peng, Phys. Rev. Lett. **68**, 3663 (1992).
17. L. M. Duan, G. Giedke, J. I. Cirac, and P. Zoller, Phys. Rev. Lett. **84**, 2722 (2000).
18. R. Simon, Phys. Rev. Lett. **84**, 2726 (2000).
19. M. J. Collett, and C. W. Gardiner, Phys. Rev. A **30**, 1386 (1984).
20. O. Pfister, S. Feng, G. Jennings, R. C. Pooser, and D. Xie, Phys. Rev. A **70**, 020302 (2004).
21. R. C. Pooser and O. Pfister, Opt. Lett. **30**, 2635 (2005).
22. O. Pfister and R. C. Pooser, private communication.